TWO- AND THREE-DIMENSIONAL BEARING CAPACITY OF FOOTINGS IN SAND

Lyamin, A.V.[1], Salgado, R.[2], Sloan, S.W.[3] and Prezzi, M.[4]

ABSTRACT

Bearing capacity calculations are an important part of the design of foundations. Many of the terms in the bearing capacity equation, as it is used today in practice, are empirical. Shape factors could not be derived in the past because three-dimensional bearing capacity computations could not be performed with any degree of accuracy. Likewise, depth factors could not be determined because rigorous analyses of foundations embedded in the ground were not possible. In this paper, the bearing capacity of strip, square, circular and rectangular foundations in sand are determined for frictional soils following an associated flow rule using finite-element limit analysis. The results of the analyses are used to propose values of the shape and depth factors for calculation of the bearing capacity of foundations in sands using the traditional bearing capacity equation. The traditional bearing capacity equation is based on the assumption that effects of shape and depth can be considered separately for soil self-weight and surcharge (embedment) terms. This assumption is not realistic, so we also propose a different form of the bearing capacity equation that does not rely on it.

[1] [1] Senior Lecturer, Department of Civil Engrg., University of Newcastle, New South Wales, Australia
[2] Professor, School of Civil Engrg., Purdue University, West Lafayette, IN, USA
[3] Professor, Department of Civil Engrg., University of Newcastle, New South Wales, Australia
[4] Assist. Professor, School of Civil Engrg., Purdue University, West Lafayette, IN, USA

INTRODUCTION

The bearing capacity equation (Terzaghi 1943, Meyerhof 1951, Meyerhof 1963, Brinch Hansen 1970) is one tool that geotechnical engineers use routinely. It is used to estimate the limit unit load q_{bL} (referred to also as the limit unit bearing capacity or limit unit base resistance) that will cause a footing to undergo classical bearing capacity failure. For a footing with a level base embedded in a level sand deposit acted upon by a vertical load, the bearing capacity equation has the following form:

$$q_{bL} = (s_q d_q) q_o N_q + 0.5(s_\gamma d_\gamma) \gamma B N_\gamma \qquad (1)$$

where N_q and N_γ are bearing capacity factors; s_q and s_γ are shape factors; d_q and d_γ are depth factors; q_o is the surcharge at the footing base level; and γ is the soil unit weight. The limit unit load is a load divided by the plan area of the footing and has units of stress. In the case of a uniform soil profile, with the unit weight above the level of the footing base also equal to γ, we have $q_0 = \gamma D$. The unit weight γ, the footing width B and the surcharge q_0 can be considered as given. The other terms of (1) must be calculated or estimated by some means.

Most theoretical work done in connection with the bearing capacity problem has been for soils following an associated flow rule. This also applies to the present paper. Until recently, the only term of (1) that was known rigorously was N_q, which follows directly from consideration of the bearing capacity of a strip footing on the surface of a weightless, frictional soil (Reissner 1924; see also Bolton 1979):

$$q_{bL} = q_o N_q \qquad (2)$$

where N_q is calculated from:

$$N_q = \frac{1+\sin\phi}{1-\sin\phi} e^{\pi \tan\phi} \quad (3)$$

Considering a strip footing on the surface of frictional soil with non-zero unit weight γ and $q_0 = 0$, the unit bearing capacity is calculated from:

$$q_{bL} = 0.5\gamma B N_\gamma \quad (4)$$

There are two equations for the N_γ in (4) that have been widely referenced in the literature:

$$N_\gamma = 1.5\ (N_q - 1) \tan\phi \quad (5)$$

by Brinch Hansen (1970) and

$$N_\gamma = 2\ (N_q + 1) \tan\phi \quad (6)$$

by Caquot and Kerisel (1953).

Although Eq. (5) was developed at a time when computations were subject to greater uncertainties, it is close to producing exact values for a frictional soil following an associated flow rule for relatively low friction angle values. It tracks well the results of slipline analyses done by Bent Hansen and Christensen (1969), Booker (1969) and Davis and Booker (1971) for a strip footing on the surface of a frictional soil with self-weight up to a ϕ value of roughly 40˚. Martin (2005) found values of N_γ based on the slipline method that are very accurate. Salgado (2008) proposed a simple equation, in a form similar to (5), that fits those values quite well:

$$N_\gamma = (N_q - 1) \tan(1.32\phi) \quad (7)$$

Equation (1) results from the superposition of the bearing capacity due to the surcharge q_0 with that due to the self-weight of the frictional soil. While the values of N_q

and N_γ satisfy a standard of rigor when used independently for the two problems for which they were developed, it is not theoretically correct to superpose the surcharge and self-weight effects (in fact, the surcharge is due to the self weight of the soil located above the footing base). Still, while not theoretically correct, the superposition of the two solutions as in (1) has been used in practice for decades. Smith (2005) has recently shown that the error introduced by superposition may be as high as 25%.

In addition to superposing the effects of surcharge and self-weight, each of the two terms on the right side of Eq. (1) contains shape and depth factors. The shape factors are used to model the problem of the bearing capacity of a footing with finite dimensions in both horizontal directions, and the depth factors are used to model the problem in which the surcharge is in reality a soil overburden due to embedment of the footing in the soil. The equations for these factors have been determined empirically based on relatively crude models (Meyerhof 1963, Hansen 1970, Vesic 1973). Table 1 and Table 2 contain the expressions more commonly used for the shape and depth factors, due to Meyerhof (1963), Brinch Hansen (1970), De Beer (1970) and Vesic (1973). The experimental data on which these equations are based are mostly due to Meyerhof (1951, 1953, 1963), who tested both prototype and model foundations. There was some additional experimental research following the work of Meyerhof. De Beer (1970) tested very small footings bearing on sand, determining limit bearing capacity from load-settlement curves using the limit load criterion of Brinch-Hansen (1963).

In this paper, we present results of rigorous analyses that we employ to obtain values of shape and depth factors for use in bearing capacity computations in sand. The shape and depth factors are determined by computing the bearing capacities of footings

of various geometries placed at various depths and comparing those with the bearing capacities of strip footings located on the ground surface for the same soil properties (unit weight and friction angle). In addition to revisiting the terms in the traditional bearing capacity equation and proposing new, improved relationships, we will also propose a different form of the bearing capacity equation, a simpler form, that does not require an assumption of independence of the self-weight and surcharge effects. This new form of the bearing capacity equation consists of one, instead of two terms.

CALCULATION OF LIMIT BEARING CAPACITY USING LIMIT ANALYSIS

Limit Analysis: background

From the time Hill (1951) and Drucker, Greenberg and Prager (1951,1952) published their ground-breaking lower and upper bound theorems of plasticity theory, on which limit analysis is based, it was apparent that limit analysis would be a tool that will provide important insights into the bearing capacity problem and other stability applications. However, the numerical techniques required for finding very close lower and upper bounds on collapse loads, thus accurately estimating the collapse loads themselves, were not available until very recently.

Limit analysis takes advantage of the lower and upper bound theorems of plasticity theory to bound the rigorous solution to a stability problem from below and above. The theorems are based on the principle of maximum power dissipation of plasticity theory, which is valid for soil following an associated flow rule. If soil does not follow an associated flow rule (the case with sands), the values of bearing capacity from limit analysis are too high. So the focus of the present paper is frictional soils following

an associated flow rule. However, for relative quantities (such as shape and depth factors), the results produced by limit analysis can be considered reasonable estimates of the quantities for sands.

Discrete formulation of lower bound theorem

The objective of a lower bound calculation is to find a stress field σ_{ij} that satisfies equilibrium throughout the soil mass, balances the prescribed surface tractions, nowhere violates the yield criterion, and maximizes Q, given in the general case by

$$Q = \int_S \mathbf{T} dS + \int_V \mathbf{X} dV \tag{8}$$

where **T** and **X** are, respectively, the surface tractions and body forces. In our analyses, body forces (soil weight) are prescribed, therefore expression (8) reduces to the first integral only.

The numerical implementation of the limit analysis theorems usually proceeds by discretizing the continuum into the set of finite elements and then using mathematical programming techniques to solve the resulting optimization problem. The choice of finite elements that can be employed to guarantee a rigorous lower bound numerical formulation is rather limited. They must be linear stress elements with the option to have discontinuous tangential stresses between adjacent elements in the mesh (Figure 1(a)). In the present analysis, these stress discontinuities are placed between all elements. If D is the problem dimensionality, then there are D+1 nodes in each element, and each node is associated with a $(D^2+D)/2$-dimensional vector of stress variables $\{\sigma_{ij}\}$, $i = 1,\ldots,D; j = i,\ldots,D$. These stresses are taken as the problem variables.

Figure 1 Three-dimensional finite elements for (a) lower bound analysis and (b) upper bound analysis.

A detailed description of the numerical formulation of lower bound theorem utilized in present study is beyond the scope of the paper and can be found in Lyamin (1999) and Lyamin & Sloan (2002a).

Discrete formulation of upper bound theorem

The objective of an upper bound calculation is to find a velocity distribution **u** that satisfies compatibility, the flow rule and the velocity boundary conditions and that minimizes the internal power dissipation, given by the integral:

$$W^{internal} = \int_V \boldsymbol{\sigma}\dot{\boldsymbol{\varepsilon}} dV \tag{9}$$

An upper bound estimate on the true collapse load can be obtained by equating $W^{internal}$ to the power dissipated by the external loads, given by:

$$W^{external} = \int_S \mathbf{T}^{\mathrm{T}}\mathbf{u} dS + \int_V \mathbf{X}^{\mathrm{T}}\mathbf{u} dV \tag{10}$$

In contrast to the lower bound formulation, there is more that one type of finite element that will enforce rigorous upper bound calculations (see e.g. Yu et al. (1994) and Makrodimopoulos and Martin (2005)). In the present work, we use the simplex finite element illustrated in Figure 1(b). Kinematically admissible velocity discontinuities are permitted at all interfaces between adjacent elements. If D is the dimensionality of the problem, then there are $D+1$ nodes in the element and each node is associated with a D-dimensional vector of velocity variables $\{u_i\}$, $i = 1,\ldots,D$. These, together with a

$(D^2+D)/2$ -dimensional vector of elemental stresses $\{\sigma_{ij}\}$, $i=1,\ldots,D;\ j=i,\ldots,D$ and a $2(D-1)$ -dimensional vector of discontinuity velocity variables $\mathbf{v}^d$ are taken as the problem variables.

A comprehensive description of the dimensionally independent formulation of upper bound formulation (suitable for cohesive-frictional materials) used to carry out computations for this research is given in Lyamin & Sloan (2002b).

Typical Meshes for Embedded Footing Problem

To increase the accuracy of the computed depth and shape factors for 3D footings, the symmetry inherent in all of these problems is fully exploited. This means that only 15°, 45° and 90° sectors are discretized for the circular, square and rectangular footings, respectively, as shown in Figures 3 through 8. These plots also show the boundary conditions adopted in the various analyses and resultant plasticity zones (shown as shaded in the figures) and deformation patterns. The 15° sector for circular footings has been used to minimize computation time. A slice with such a thickness can be discretized using only one layer of well-shaped elements, while keeping the error in geometry representation below 1% (which is approximately 5 times less than the accuracy of the predicted collapse load, as we will see later).

Figure 2 Typical lower-bound mesh and plasticity zones for circular footings.

Figure 3 Typical upper-bound mesh and deformation pattern for circular footings.

Figure 4 Typical lower-bound mesh and plasticity zones for rectangular footings.

Figure 5 Typical upper-bound mesh and deformation pattern for rectangular footings.

Figure 6 Lower-bound mesh and plasticity zones for strip footing with D/B = 0.2, 1.0 and 2.0.

Figure 7 Upper-bound mesh and deformation pattern for strip footing with D/B = 0.2, 1.0 and 2.0.

For the lower-bound meshes, special extension elements are included to extend the stress field over the semi-infinite domain (thus guaranteeing the solutions obtained are rigorous lower bounds on the true solutions (Pastor (1978)). To model the embedded conditions properly, the space above the footing was filled with soil. At the same time, the model includes a gap between the top of the footing and this fill; this gap is supported by normal hydrostatic pressure, as shown in the enlarged diagrams of Figure 2 - Figure 7. Rough conditions are applied at the top and bottom of the footing by prescribing zero tangential velocity for upper bound calculations and specifying no particular shear stresses for lower bound calculations (that is, the yield criterion is operative between the footing and the soil in the same way as it is operative within the soil). This modeling strategy is geometrically simple, producing a result that is close to the desired quantity (pure unit base resistance) with only a slight conservative bias when compared with other possible modeling options, shown in Figure 8.

In order to illustrate the differences between results from the different options, we performed a model comparison study, which is summarized in Table 3. For each option, the lower (LB), upper (UB) and average (Avg) values of collapse pressure were computed using FE meshes similar to those shown in Figure 6 and Figure 7. From the

results presented in Table 3, it is apparent that a simple "rigid-block" model is on the unsafe side when "rough" walls are assumed and too conservative when "smooth" walls are assumed when compared with realistically shaped footings. On the other hand, the "rigid-plate" model with hydrostatically supported soil above the plate is safe for all considered D/B ratios and has the lowest geometric complexity (which is especially helpful in modeling 3D cases). Note, however, that the differences between the results of all the analyses are not large, even for the maximum D/B value considered in the calculations. The difference between all considered footing geometries and wall/soil interface conditions (for a rough base in all cases) is not greater than 14%. If we exclude the "rigid-block" model, this figure drops to just 5% for the maximum D/B ratio considered.

Figure 8 Modeling options for embedded 2D footing.

DETERMINATION OF THE TRADITIONAL BEARING CAPACITY EQUATION TERMS

Range of Conditions Considered in the Calculations

Our goal in this section is to generate equations for shape and depth factors that will perform the same function as the equations in Table 1 and Table 2, but will do so with greater accuracy. The range of friction angles of sands is from roughly 27 to about 45 degrees (for square and circular footings) and from 27 to about 50 degrees (for strip footings, to which plane-strain friction angles apply). Accordingly, the frictional soils considered in our calculations have ϕ = 25, 30, 35, 40, and 45 degrees.

We are interested in both circular and square footings. In practice, most rectangular footings have L/B of no more than 4, where L and B are the two plan dimensions of the footing. Accordingly, our calculations are for footings with L/B = 1, 2, 3, and 4. The maximum embedment for shallow foundations is typically taken as D = B. We more liberally established 2B as the upper limit of the D/B range considered in our calculations. The embedment ratios we considered were 0.1, 0.2, 0.4, 0.6, 0.8, 1 and 2.

Determination of N_γ

The very first step in this process of analysis of the bearing capacity equation is the determination of N_γ, which requires the determination of lower and upper bounds on the bearing capacity of a strip footing on the surface of a frictional soil. Equation (1) is rewritten for this case as:

$$q_{bL} = \frac{1}{2}\gamma B N_\gamma \qquad (11)$$

Calculations were done with $\gamma = 1$ and $B = 2$ so that q_{bL} resulted numerically equal to N_γ. The lower and upper bound values of N_γ calculated in this way using limit analysis are shown in Table 4 and Figure 9, which also show the values calculated using (5), (6), and (7). For completeness, the table shows also the value of N_q for each friction angle. It can be seen that the values of N_γ calculated using (5) fall between the lower and upper bounds on N_γ for ϕ values lower than 40° and then fall below the lower bound for $\phi \geq 40°$. Values of N_γ calculated using (7) fall within the range determined by lower- and upper-bound solutions for all ϕ values of interest. On the other hand, N_γ calculated using (6) results too high. So this equation, the Caquot and Kerisel (1953) equation, is not correct, and its use should be discouraged.

Figure 9 The bearing capacity factor N_γ from upper and lower bound analyses and from the equations due to Brinch-Hansen and to Caquot and Kerisel.

Determination of the Depth Factors

The depth factor d_γ was taken as 1 by both Vesic (1973) and Brinch Hansen (1970), as seen in Table 2. Conceptually, a $d_\gamma = 1$ means that the N_γ term refers only to the slip mechanism that forms below the base of the footing. This means that the effects of the portion of the mechanism extending above the base of the footing are fully captured by the depth factor d_q. In this section, we take $d_\gamma = 1$ as well.

For the determination of d_q, we consider a strip footing at depth. For this case, (1) becomes:

$$\begin{aligned} q_{bL} &= d_q q_o N_q + 0.5\gamma B N_\gamma \\ &= d_q \gamma D N_q + 0.5\gamma B N_\gamma \end{aligned} \qquad (12)$$

The lower and upper bounds on the second term on the right side of (12) and indeed the nearly exact value of it are known, as discussed earlier. The corresponding values of d_q can then be calculated from (12), rewritten as:

$$d_q = \frac{q_{bL} - 0.5\gamma B N_\gamma}{q_0 N_q} \qquad (13)$$

The results of these calculations, given in Table 5, show clearly that the depth factor d_q does not approach 1 when $D/B \rightarrow 0$, as would be suggested by the expressions

given in Table 2. On the contrary, it increases with decreasing D/B. This fact can be explained by the inadequacy of the logic of superposition and segregation of the different contributions to bearing capacity. Indeed, the theory of the depth factor d_q is that it would correct for the shear strength of the soil located above the level of the footing base, which disappears upon the replacement of the overburden soil by a surcharge. The reality of the depth factor d_q, computed using (13), is that it accumulates two contributions. The first contribution is the intended one: the contribution of the shear strength of the soil located above the level of the footing base, which is lost upon its replacement by an equivalent surcharge. The second contribution results from the fact that replacing the soil above the footing base by an equivalent surcharge produces a different response of the soil below the footing base. Note that this is contrary to the assumption that the response of the soil below the footing base is independent of what happens above it (which is the logic behind making $d_\gamma = 1$). Figure 10 shows, using upper bound calculations, that the power dissipated by the velocity field in the presence of the body forces above the level of an embedded footing is greater than the power dissipated by the same footing placed at the surface in the presence of an equivalent surface surcharge. This is seen by the larger extent of the collapse mechanism in the presence of soil above the footing base compared with that for an equivalent surcharge. To visualize this, we can compare Figure 10(a) and Figure 10(b). We can see from this comparison that there is no energy dissipated to the right side of line A-A for the case in which a surcharge load is used; so A-A marks the boundary of the collapse mechanism in that case. However, there is considerable energy dissipated to the right of A-A when soil is used instead of an equivalent surcharge. So the fact that there is a soil-on-soil

interaction at the level of the base of the footing as opposed to simply a surcharge does have an impact on what happens below the footing base level. When that is ignored by making $d_\gamma = 1$, the effects appear in the value of d_q.

Figure 10 Illustration of difference in work done by external forces in two cases: (a) an equivalent surcharge is used to replace the soil above the base of the footing and (b) the footing is modeled as an embedded footing.

The depth factor d_q is plotted in Figure 11 with respect to the depth of embedment for the five friction angles examined: 25, 30, 35, 40 and 45 degrees. The following equation fits well the numbers for $\phi = 25$ to 45° in the D/B range from 0 to 2:

$$d_q = 1 + (0.0036\phi + 0.393)\left(\frac{D}{B}\right)^{-0.27} \qquad (14)$$

Figure 11 Depth factor d_q versus depth for various friction angles.

Determination of s_γ

For a square, circular or rectangular footing on the surface of a soil deposit, (1) becomes:

$$q_{bL} = 0.5\gamma B s_\gamma N_\gamma \qquad (15)$$

Given that $0.5\gamma B = 1$ in our calculations, the calculated bounds on q_{bL} are bounds on $s_\gamma N_\gamma$. These values are shown in Table 6. The lower bound s_γ is obtained by dividing the lower bound $s_\gamma N_\gamma$ by the corresponding N_γ value from Martin (2005), shown in the

second column of the table (and approximated by Eq.(7)). The bounds on s_γ are also given in Table 6.

Taking the average of the upper and lower bounds as our best estimate of s_γ would be appropriate if the lower and upper bounds converged to a common value at the same rate with increasing mesh refinement. It was observed, however, particularly for rectangular footings (for which computation accuracy drops significantly with increasing values of L/B because of the coarser mesh that must be used), that the convergence rates are different for lower and upper bound calculations. A convergence study was performed for each of the 3D shapes considered for footings in the present paper by using progressively finer meshes. The convergence rates are approximately the same for lower and upper bound computations for the plane-strain case, as shown in Figure 12(a), but the convergence rates for bounds on the bearing capacity of footings with finite values of L are significantly different (see Figure 12(b)). This means that taking the average of the two bounds does not give the best estimate of s_γ, which is obtained instead from the asymptotes computed for the lower and upper bound solutions. If, say LB_1 and LB_2 are two lower bound estimates on some quantity obtained with two different FE meshes, and UB_1 and UB_2 are two upper bound solutions from two meshes like the two lower bound meshes, then the ratio of convergence rates of bounding solutions can be written as $\alpha = \Delta\mathrm{UB}/\Delta\mathrm{LB} = \left(\mathrm{UB}_1 - \mathrm{UB}_2\right)/\left(\mathrm{LB}_2 - \mathrm{LB}_1\right)$. Given that information, the point of intersection of LB and UB plots (which we may call a weighted-average approximation to the collapse load) can be estimated as $\mathrm{PI} = w_{\mathrm{LB}}\mathrm{LB}_1 + w_{\mathrm{UB}}\mathrm{UB}_1$, where $w_{\mathrm{LB}} = \alpha/(1+\alpha)$, $w_{\mathrm{UB}} = 1/(1+\alpha)$. To assess the level of accuracy which can be expected from this approach, N_γ was calculated using the above

formula and coarse meshes with the same pattern as the cross sections of the 3D meshes used for circular and rectangular footings. The results of this test are presented in the last two columns of Table 4. The coarse meshes used in the N_γ computations result in a wide gap between bounds (as observed in some of the 3D calculations), but the weighted average estimates, $N_{\gamma,w}$, are quite close to the exact values of N_γ.

Figure 12 Convergence rates in the case of strip (a) and circular (b) footings.

Figure 13 shows the results of calculations for surface footings. These results suggest that there are no easy generalizations, based on simple physical rationalizations, as to what the shape factor s_γ should be. It can be greater or less than one, and increase or decrease with increasing B/L. Note that s_γ is both less than 1 and decreases with increasing B/L for $\phi = 25^\circ$ and $\phi = 30^\circ$, while it is greater than 1 and increases with increasing B/L for $\phi = 35^\circ$ through 45° (which are the cases of greater interest in practice). Note also that the value of ϕ that would lead to $s_\gamma = 1$ for all values of B/L is slightly greater than 30°. Using the Martin (2005) N_γ values as reference, our shape factors for $\phi = 35^\circ$ through 45° are 15 to 20% lower than the values of Erickson and Drescher (2002), obtained using FLAC. A final interesting observation is that the variation of s_γ with B/L is essentially linear for all ϕ values considered. Zhu and Michalowski (2005) also observed a linear relationship between s_γ and B/L for values of B/L less than approximately 0.3, but a more complex trend for B/L > 0.3. Their s_γ values were also less than 1 for $\phi < 30^\circ$ and greater than 1 for $\phi > 30^\circ$.

The following equation approximates quite well the shape factor for surface footings calculated using the present analysis:

$$s_\gamma = 1 + (0.0336\phi - 1)\frac{B}{L} \qquad (16)$$

Figure 13 Variation of shape factor s_γ for surface footings with respect to B/L.

In deriving Eq. (16), we used the bearing capacity of the square footing for B/L = 1. The bearing capacity of the circular footing is slightly greater: the shape factor for a circular footing can be obtained by multiplying that of the square footing in the same conditions by $1 + 0.002\phi$.

There are a number of physical processes whose interaction produces the bearing capacities of strip and finite-size footings. Two competing effects are the larger slip surface area for finite-size footings versus the larger constraint/confinement imposed on the mechanism in the case of strip footings. The larger slip surface area (or larger plastic area) that would lead to $s_\gamma > 1$ was observed for circular footings by Bolton and Lau (1993) and by Zhu and Michalowski (2005) using finite element analysis; it was earlier hypothesized by Meyerhof (1963). In contrast, Vesic (1973) and Brinch-Hansen (1970) proposed expression yielding $s_\gamma < 1$ (refer to Table 1).

Based on our results, it would appear that, for sufficiently low ϕ values, the greater constraint imposed on slip mechanisms in the case of the upper bound or greater confinement imposed on the stress field in the case of the lower bound method more than compensates for the smaller slip surface area, resulting in $s_\gamma < 1$. But for ϕ values greater

than about 30 degrees, which is the range we tend to see in practice, the larger slip surface area dominates, and $s_\gamma > 1$. This contrasts with the Vesic (1973) and Brinch-Hansen (1970) equations, popular in practice, which give $s_\gamma < 1$ no matter what. The physical reasoning that has been advanced in support of these equations is that square and rectangular footings generate smaller mean stress values below the footing, which in turn lead to lower shear strength than that available for a strip footing under conditions of plane strain. However, that argument applies only for footings placed on the surface of identical sand deposits, with the same relative density, for which q_{bL} will indeed be larger for a plane-strain footing (for which ϕ will be higher) than for a circular or rectangular footing with the same width B. If equations in terms of ϕ are used in calculations, that difference should not be accounted for by making $s_\gamma < 1$, but rather by taking due account of the lower ϕ for footings in conditions other than plane-strain conditions. So a physical reasoning in which a comprehensive accounting of all the processes in place is not done may lead to the wrong conclusion, as in the case that has been made for s_γ less than one for equations written in terms of ϕ.

Determination of s_q

The final factor to determine is the shape factor s_q. Now equation (1) is used directly. We can rewrite it so that s_q is expressed as:

$$s_q = \frac{q_{bL} - 0.5\left(s_\gamma d_\gamma\right)\gamma B N_\gamma}{d_q q_0 N_q} \qquad (17)$$

It is clear that we must know s_γ in order to calculate s_q. Here we make the operational assumption that s_γ is independent of depth. When we make this assumption,

we implicitly decide that all of the depth-related effects that were not reflected in the values of d_q because they are coupled with the footing shape, will be captured by s_q. Calculations are summarized for square footings in Table 7. The results are shown graphically for all values of L/B in Figure 14. Note that s_q is not defined at D = 0, when $q_0 = 0$, and that it must equal 1 for B/L = 0 (plane strain). The mathematical form

$$s_q = 1 + f_{q1}\left(\phi, \frac{D}{B}\right)\left(\frac{B}{L}\right)^{f_{q2}\left(\phi, \frac{D}{B}\right)} \tag{18}$$

can be used to fit the results, where functions f_{q1} and f_{q2} of ϕ and D/B must be found such that the fit is optimal. For low ϕ values and B/L ≤ 0.5, the behavior is very nearly linear, with f_{q2} being approximately equal to 1. The following expression was fit to the limit analysis results:

$$s_q = 1 + \left(0.098\phi - 1.64\right)\left(\frac{D}{B}\right)^{0.7-0.01\phi}\left(\frac{B}{L}\right)^{1-0.16\left(\frac{D}{B}\right)} \tag{19}$$

For small D/B values, Eq. (19) is approximately linear in B/L. The equation, for B/L = 1, applied to square footings. For circular footings, the s_q of Eq. (19) must be multiplied by an additional factor equal to $1 + 0.0025\phi$.

Figure 14 Shape factor s_q versus B/L for various for D/B ranging from 0.1 to 2 and (a) ϕ = 25º, (b) ϕ = 30º, (c) ϕ = 35º, (d) ϕ = 40º, (e) ϕ = 45º.

Alternative Form of Bearing Capacity Equation for Sands

As noted in both the present paper and in Salgado et al. (2004) for clays, shape and depth factors are interdependent, in contrast with the assumption that is necessary to propose a bearing capacity equation in the form of Eq. (1). While in the preceding sub-

sections we retained the traditional form of the bearing capacity equation and determined expressions for s_q, s_γ, d_q and d_γ that take due account of the interdependence of all quantities, we will now explore an alternative form of the bearing equation that is simpler and does not attempt to dismember bearing capacity into artificial components.

A much simplified form of the bearing capacity equation can be proposed now that numerical limit analysis allows treatment of the soil overburden as what it really is: a soil, not a surcharge. When we do that, the N_q term completely disappears and we are left with:

$$q_{bL} = \frac{1}{2}\gamma B s_\gamma^* d_\gamma^* N_\gamma \tag{20}$$

As before, we follow tradition and separate depth and shape effects in (20) by using two factors (d_γ^* and s_γ^*). If we set d_γ^* as a function of depth only, we can use (20) to calculate the bearing capacity of strip footings, for which s_γ^* is 1. For rectangular and circular footings, we find that s_γ^* depends not only on B/L but also on depth.

Using the same data as before, we can calculate d_γ^* by using:

$$d_\gamma^* = \frac{q_{bL,strip}\Big|_{\frac{D}{B}}}{q_{bL,strip}\Big|_{\frac{D}{B}=0}} \tag{21}$$

Figure 15 shows the depth factor, calculated as per eq. (21), versus D/B for the five values of friction angle considered. The relationship between d_γ^* and D/B is almost perfectly linear. The following equation represents the straight lines shown in the figure quite well:

$$d_\gamma^* = 1 + \left(8.404 - 0.151\phi\right)\frac{D}{B} \tag{22}$$

where the friction angle is given in degrees.

Figure 15 Depth factor d_γ^*.

The shape factor is calculated for a given D/B value as:

$$s_\gamma^* = \frac{q_{bL}\left|_{\frac{B}{L}}\right.}{q_{bL,strip}} \tag{23}$$

The value of s_γ^* for D/B = 0 is obviously the same as s_γ, given by Eq. (16). The ratio of s_γ^* to s_γ is therefore a function of D/B and B/L that takes the value of 1 at D/B = 0. The following equation captures this relationship quite well:

$$\frac{s_\gamma^*}{s_\gamma} = 1 + \left[0.31 + 0.95\frac{B}{L}\right]\left[2.63 + 0.023\phi\right]\left(\frac{D}{B}\right)^{1.15-0.54\frac{B}{L}} \tag{24}$$

In deriving the depth and shape factors, we assumed d_γ* to be independent of shape, with the result that the shape factor depends on depth, as clearly shown by (24). When we multiply together the shape factor and depth factor in (20), the issue of whether it is the depth factor that depends on B/L or the shape factor that depends on D/B disappears. In other words, the same final equation would have resulted had we assumed the shape factor to be independent of depth and the depth factor to depend on B/L, or, put more simply, had we assumed a single correction factor, function of ϕ, B/L and D/B.

SUMMARY AND CONCLUSIONS

We have performed rigorous upper and lower bound analyses of circular, rectangular and strip footings in sand. These analyses provided ranges within which the exact collapse loads for the footings are to be found. These analyses are possible at this time because of efficient algorithms for optimization of stress fields for lower bound analysis and velocity fields for upper bound analysis.

We have also examined the traditional bearing capacity equation and the underlying assumptions of superposition of surcharge and self-weight terms and independence of shape factors from depth and depth factors from shape of the footings. We have found that these assumptions are not valid. We proposed new shape and depth factors that do account for the interdependence of all the terms. Additionally, the derivation of these factors did not require making the assumption of superposition.

An alternative bearing capacity equation with a single term is simpler than the traditional form of the bearing capacity equation. For surface strip footings, the equation reduces to the traditional $\frac{1}{2}\gamma B N_\gamma$ form. Depth is accounted for by multiplying this term by a depth factor d_γ^*, and shape by multiplication by a shape factor s_γ^*. As shape and depth are not truly independent, the final equation can be viewed as simply the basic $\frac{1}{2}\gamma B N_\gamma$ term multiplied by functions of B/L and D/B.

REFERENCES

Bolton (1979). "A Guide to Soil Mechanics." Macmillan, London, 439 pages; reprinted by Chung Hwa Books, and published by M.D. and K. Bolton in 1998.

Bolton, M.D. and Lau,C.K. (1993). "Vertical Bearing Capacity Factors for Circular and Strip Footings on Mohr-Coulomb Soil." Canadian Geotechnical Journal, 30, 1024-1033.

Booker, J.R. (1969). "Applications of Theories of Plasticity to Cohesive Frictional Soils." Ph.D. thesis, Sydney University.

Brinch Hansen, J. (1970). "A Revised and Extended Formula for Bearing Capacity." The Danish Geotechnical Institute, Bulletin No. 28.

Caquot, A. and Kerisel, J. (1953). "Sur le terme de surface dans le calcul des fondations en milieu pulverent." Proc. 3rd ICSMFE, Zurich, 1, pp. 336-337.

Davis, E.H. and Booker, J.R. (1971). "The bearing capacity of strip footings from the standpoint of plasticity theory". In: Proceedings of the first Australian-New Zealand Conference on Geomechanics, Melbourne, 275-282

De Beer, E.E. (1970). "Experimental Determination of the Shape Factors and the Bearing Capacity Factors of Sand." Geotechnique, 20(4), pp. 387-411.

Drucker, D.C., Greenberg, W. and Prager, W. (1951). "The Safety Factor of an Elastic-Plastic Body in Plane Strain." Transactions of the ASME, Journal of Applied Mechanics, 73, 371.

D C Drucker, W Prager and H J Greenberg (1952). "Extended limit design theorems for continuous media." Quarterly of Applied Mathematics, 9, 381-389.

Erickson, H.L., and Drescher, A. (2002). "Bearing capacity of circular footings." J. Geotech. Geoenv. Eng, ASCE, 128, 38-43.

Hansen, B and Christiansen. (1969). "Discussion of theoretical bearing capacity of very shallow footings." by A.L. Larkin. Journal of Soil Mechanics and Foundations Division (ASCE) 95 (SM6), 1568-1567.

R. Hill (1951). "On the state of stress in a plastic-rigid body at the yield point." Phil. Mag. Vol 42, 868-875.

Lyamin AV. (1999). Three-dimensional Lower Bound Limit Analysis Using Nonlinear Programming, *PhD Thesis*, Department of Civil, Surveying and Environmental Engineering, University of Newcastle, NSW.

Lyamin AV, Sloan SW. (2002a). "Lower bound limit analysis using nonlinear programming." *International Journal for Numerical Methods in Engineering*; 55, 573-611.

Lyamin AV, Sloan SW. (2002b). "Upper bound limit analysis using linear finite elements and nonlinear programming." *International Journal for Numerical and Analytical Methods in Geomechanics,* 26(2), 181-216.

Martin, C. M. (2001). "Vertical Bearing Capacity of Skirted Circular Foundations on Tresca Soil. " Proc. 15th ICSMGE, Istanbul, Vol. 1, 743–746.

Martin, C.M. (2005). "Exact bearing capacity calculations using the method of characteristics. " Proc. 11th Int. Conf. of IACMAG, Turin, Vol. 4, pp 441-450.

Meyerhof, G.G. (1951). "The Ultimate Bearing Capacity of Foundations" Geotechnique, 2(4), 301-332.

Meyerhof, G.G. (1963). "Some Recent Research on bearing Capacity of Foundations." Canadian Geotech. J., 1, 16-26 (1963).

Prandtl, L. (1920). "Über die Härte Plasticher Körper." Nachr. Ges. Wiss. Gött., Math-Phys. Kl., 12, 74-85.

Prandtl, L. (1921). "Eindringungsfestigkeit und Festigkeit von Schneiden." Zeit F. Angew. Math. U. Mech., 1, 15.

Reissner, H. (1924). "Zum Erddruckproblem." Proc. 1st International Congress for Applied Mechanics, Delft, 295-311.

Salgado, R., Lyamin, A., Sloan, S. and Yu, H.S. (2004). "Two- and Three-dimensional Bearing Capacity of Footings in Clay." *Geotechnique* 54(5), 297-306.

Skempton, A.W. (1951). "The Bearing Capacity of Clays." Building Research Congress, Div. I, 180.

Smith, C.C. (2005). "Complete Limiting Stress Solutions for the Bearing Capacity of Strip Footings on a Mohr Coulomb Soil." Geotechnique, 55, No. 8, 607-612.

Terzaghi, K. (1943). "Theoretical Soil Mechanics." Wiley, New York, 510 pp.

Ueno, K., Miura, K. and Maeda, Y. (1998). "Prediction of Ultimate Bearing Capacity of Surface Footings with Regard to Size Effects." Soils and Foundations, 38(3), pp. 165-178.

Vesic, A.S. (1973). "Analysis of Ultimate Loads of Shallow Foundations." J. of Soil Mech, Div., 99(SM1), 45-73.

Pastor, J. (1978). “Analyse limite: determination de solutions statiques completes – Application au talus vertical. European Journal of Mechanics *A/Solids*, 2:176-196.

Makrodimopoulos, A. and Martin, C. M. (2005). Upper bound limit analysis using simplex strain elements and second-order cone programming. Technical Report 2288/2005, University of Oxford.

Yu, H. S., Sloan, S. W., and Kleeman, P. W. (1994). A quadratic element for upper bound limit analysis. Engineering Computations, 11:195–212.

Zhu, M. and Michalowski, R.L. (2005). "Shape factors for limit loads on square and rectangular footings." *Journal of Geotechnical and Geoenvironmental Engineering*, 131, No. 2, 223-231.

Table 1. Commonly used expressions for shape factors**.**

q_0 term	γ term
Meyerhof (1963)	
$s_q = 1 + 0.1N\frac{B}{L}$	$s_\gamma = 1 + 0.1N\frac{B}{L}$
Brinch -Hansen (1970)	
$s_q = 1 + \frac{B}{L}\sin\phi$	$s_\gamma = 1 - 0.4\frac{B}{L} \geq 0.6$
Vesic (1973)	
$s_q = 1 + \frac{B}{L}\tan\phi$	$s_\gamma = 1 - 0.4\frac{B}{L} \geq 0.6$

N = flow number = $\tan^2(45+\phi/2)$

Table 2. Commonly used expressions for depth factors**.**

q_0 term	γ term
Meyerhof (1963)	
$d_q = 1 + 0.1\sqrt{N}\frac{D}{B}$	$d_\gamma = 1 + 0.1\sqrt{N}\frac{D}{B}$
Brinch Hansen (1970) and Vesic (1973)	
$D/B \le 1$	$d_\gamma = 1$
$d_q = 1 + 2\tan\phi(1-\sin\phi)^2\frac{D}{B}$	
$D/B > 1$	
$d_q = 1 + 2\tan\phi(1-\sin\phi)^2\tan^{-1}\frac{D}{B}$	

N = flow number = $\tan^2(45+\phi/2)$

Table 3. Bearing capacities of different 2D models of embedded footing.

$\frac{D}{B}$	T-bar footing						T-cone footing						Rigid Block footing						Rigid Plate (fixed top)			Rigid Plate (top support)		
	rough walls			smooth walls			rough walls			smooth walls			rough walls			smooth walls								
	LB	UB	Avg	LB	UB	Avg	LB	UB	Avr	LB	UB	Avg	LB	UB	Avg	LB	UB	Avg	LB	UB	Avg	LB	UB	Avg
0.4													77.1	85.6	81.4	75.7	83.3	79.5	77.1	84.8	80.9	76.5	84.0	80.2
1.0	134.1	150.2	142.1	132.2	147.6	139.9	133.4	148.4	140.9	133.3	148.3	140.8	138.1	154.8	146.5	130.0	144.7	137.3	134.3	149.3	141.8	132.0	146.6	139.3
2.0	241.7	271.0	256.3	236.4	262.7	249.6	241.6	269.2	255.4	237.4	263.1	250.3	258.8	289.3	274.1	228.9	253.8	241.4	239.5	265.0	252.3	232.9	257.9	245.4

Table 4. Values of N_q and of N_γ calculated using limit analysis and equations (5), (6) and (7).

ϕ	N_q	N_γ – Eq. (5)	N_γ – Eq. (6)	N_γ – Eq. (7)	N_γ (Martin)	N_γ (LB)	N_γ (UB)	Error, %	$N_{\gamma,w}$	Error, %
25°	10.66	6.76	10.88	6.49	6.49	6.44	7.09	4.80	6.72	3.57
30°	18.40	15.07	22.40	14.75	14.75	14.57	15.90	4.36	15.51	5.18
35°	33.30	33.92	48.03	34.48	34.48	33.81	36.98	4.48	35.01	1.54
40°	64.20	79.54	109.41	85.47	85.57	82.29	91.86	5.50	89.94	5.10
45°	134.87	200.81	271.75	234.2	234.21	221.71	255.44	7.07	242.96	3.74

Table 5. Depth factor d_q (obtained from the weighted average of the lower and upper bounds on strip footing bearing capacity) for D = 0.1 to 2B and ϕ = 25°-45°.

ϕ	D/B	q_{bl} (LB)	q_{bl} (UB)	q_{bl}	q_o	q_oN_q	$0.5\gamma BN_\gamma$	d_q	Error %
25°	0.1	10.62	11.07	10.65	0.2	2.13	6.49	1.95	2.11
	0.2	13.90	14.41	13.94	0.4	4.26	6.49	1.75	1.83
	0.4	19.99	20.73	20.05	0.8	8.53	6.49	1.59	1.85
	0.6	25.92	26.87	25.99	1.2	12.79	6.49	1.52	1.83
	0.8	31.93	33.16	32.02	1.6	17.06	6.49	1.50	1.92
	1.0	38.08	39.67	38.20	2.0	21.32	6.49	1.49	2.08
	2.0	70.85	73.95	71.09	4.0	42.65	6.49	1.51	2.18
30°	0.1	21.90	23.07	22.06	0.2	3.68	14.75	1.99	2.65
	0.2	27.59	28.88	27.76	0.4	7.36	14.75	1.77	2.32
	0.4	38.07	39.91	38.32	0.8	14.72	14.75	1.60	2.40
	0.6	48.37	50.67	48.68	1.2	22.08	14.75	1.54	2.36
	0.8	58.76	61.47	59.13	1.6	29.44	14.75	1.51	2.29
	1.0	69.21	72.81	69.70	2.0	36.80	14.75	1.49	2.58
	2.0	125.44	132.52	126.40	4.0	73.60	14.75	1.52	2.80
35°	0.1	46.99	50.04	47.63	0.2	6.66	34.48	1.98	3.20
	0.2	57.29	60.89	58.05	0.4	13.32	34.48	1.77	3.10
	0.4	76.49	81.09	77.46	0.8	26.64	34.48	1.61	2.97
	0.6	95.11	100.74	96.30	1.2	39.96	34.48	1.55	2.92
	0.8	113.46	120.65	114.98	1.6	53.27	34.48	1.51	3.13
	1.0	132.07	140.95	133.95	2.0	66.59	34.48	1.49	3.31
	2.0	232.93	248.15	236.15	4.0	133.18	34.48	1.51	3.22
40°	0.1	108.09	117.84	111.43	0.2	12.84	85.57	2.01	4.37
	0.2	128.53	139.60	132.32	0.4	25.68	85.57	1.82	4.18
	0.4	165.62	179.30	170.31	0.8	51.36	85.57	1.65	4.02
	0.6	201.32	217.82	206.98	1.2	77.03	85.57	1.58	3.99
	0.8	237.00	256.76	243.77	1.6	102.71	85.57	1.54	4.05
	1.0	273.13	295.84	280.91	2.0	128.39	85.57	1.52	4.04
	2.0	463.99	499.86	476.28	4.0	256.78	85.57	1.52	3.77
45°	0.1	277.45	312.38	290.39	0.2	26.97	234.21	2.08	6.01
	0.2	321.10	360.05	335.53	0.4	53.95	234.21	1.88	5.80
	0.4	401.50	447.54	418.56	0.8	107.90	234.21	1.71	5.50
	0.6	479.00	531.41	498.42	1.2	161.85	234.21	1.63	5.26
	0.8	555.46	614.58	577.37	1.6	215.80	234.21	1.59	5.12
	1.0	631.77	696.15	655.63	2.0	269.75	234.21	1.56	4.91
	2.0	1019.70	1117.08	1055.79	4.0	539.50	234.21	1.52	4.61

Table 6. Lower and upper bounds on shape factors and their weighted averages.

Circular footing										
ϕ	N_γ	$s_\gamma N_\gamma$ (LB)	s_γ (LB)	$s_\gamma N_\gamma$ (UB)	s_γ (UB)	ΔUB/ΔLB	w (LB)	w (UB)	$s_\gamma N_{\gamma,w}$	$S_{\gamma,w}$
25°	6.49	5.65	0.87	8.26	1.27	3.57	0.78	0.22	6.22	0.96
30°	14.75	14.10	0.96	19.84	1.35	2.69	0.73	0.27	15.65	1.06
35°	34.48	37.18	1.08	52.51	1.52	2.69	0.73	0.27	41.33	1.20
40°	85.57	106.60	1.25	157.21	1.84	2.41	0.71	0.29	121.45	1.42
45°	234.21	338.00	1.44	539.22	2.30	2.31	0.70	0.30	398.80	1.70
Square footing										
ϕ	N_γ	$s_\gamma N_\gamma$ (LB)	s_γ (LB)	$s_\gamma N_\gamma$ (UB)	S_γ (UB)	ΔUB/ΔLB (asm)	w (LB)	w (UB)	$s_\gamma N_{\gamma,w}$	$S_{\gamma,w}$
25°	6.49	5.10	0.79	9.05	1.39	4.15	0.81	0.19	5.87	0.90
30°	14.75	12.67	0.86	21.82	1.48	4.03	0.80	0.20	14.49	0.98
35°	34.48	32.96	0.96	58.60	1.70	3.54	0.78	0.22	38.61	1.12
40°	85.57	91.04	1.06	184.73	2.16	3.30	0.77	0.23	112.84	1.32
45°	234.21	277.00	1.18	683.09	2.92	3.63	0.78	0.22	364.79	1.56
Rectangular footing, L/B=1.2										
ϕ	N_γ	$s_\gamma N_\gamma$ (LB)	s_γ (LB)	$s_\gamma N_\gamma$ (UB)	S_γ (UB)	ΔUB/ΔLB (asm)	w (LB)	w (UB)	$s_\gamma N_{\gamma,w}$	$S_{\gamma,w}$
25°	6.49	4.77	0.73	13.60	2.10	6.80	0.87	0.13	5.90	0.91
30°	14.75	11.57	0.78	30.31	2.05	5.22	0.84	0.16	14.58	0.99
35°	34.48	28.48	0.83	79.11	2.29	3.93	0.80	0.20	38.75	1.12
40°	85.57	71.91	0.84	268.98	3.14	4.44	0.82	0.18	108.14	1.26
45°	234.21	194.70	0.83	1013.72	4.33	3.97	0.80	0.20	359.59	1.54
Rectangular footing, L/B=2										
ϕ	N_γ	$s_\gamma N_\gamma$ (LB)	s_γ (LB)	$s_\gamma N_\gamma$ (UB)	S_γ (UB)	ΔUB/ΔLB (asm)	w (LB)	w (UB)	$s_\gamma N_{\gamma,w}$	$S_{\gamma,w}$
25°	6.49	5.10	0.79	12.47	1.92	5.99	0.86	0.14	6.15	0.95
30°	14.75	12.10	0.82	27.57	1.87	4.44	0.82	0.18	14.94	1.01
35°	34.48	28.87	0.84	71.77	2.08	3.78	0.79	0.21	37.84	1.10
40°	85.57	71.10	0.83	233.92	2.73	4.60	0.82	0.18	100.19	1.17
45°	234.21	189.60	0.81	870.00	3.71	5.38	0.84	0.16	296.19	1.26
Rectangular footing, L/B=3										
ϕ	N_γ	$s_\gamma N_\gamma$ (LB)	s_γ (LB)	$s_\gamma N_\gamma$ (UB)	S_γ (UB)	ΔUB/ΔLB (asm)	w (LB)	w (UB)	$s_\gamma N_{\gamma,w}$	$S_{\gamma,w}$
25°	6.49	5.16	0.80	11.74	1.81	4.85	0.83	0.17	6.28	0.97
30°	14.75	12.08	0.82	26.13	1.77	3.85	0.79	0.21	14.98	1.02
35°	34.48	28.11	0.82	68.69	1.99	3.65	0.78	0.22	36.84	1.07
40°	85.57	67.36	0.79	214.76	2.51	4.45	0.82	0.18	94.41	1.10
45°	234.21	174.90	0.75	786.85	3.36	5.10	0.84	0.16	275.26	1.18
Rectangular footing, L/B=4										
ϕ	N_γ	$s_\gamma N_\gamma$ (LB)	s_γ (LB)	$s_\gamma N_\gamma$ (UB)	S_γ (UB)	ΔUB/ΔLB (asm)	w (LB)	w (UB)	$s_\gamma N_{\gamma,w}$	$S_{\gamma,w}$
25°	6.49	5.15	0.79	11.30	1.74	3.97	0.80	0.20	6.39	0.98
30°	14.75	11.98	0.81	25.20	1.71	3.40	0.77	0.23	14.98	1.02
35°	34.48	27.50	0.80	67.50	1.96	3.75	0.79	0.21	35.92	1.04
40°	85.57	64.78	0.76	203.40	2.38	4.17	0.81	0.19	91.58	1.07
45°	234.21	165.00	0.70	739.00	3.16	5.19	0.84	0.16	257.66	1.10

Table 7. Lower and upper bounds on s_q for square footing and their weighted averages.

ϕ	D/B	q_{bl} (LB)	q_{bl} (UB)	$q_{bl,w}$	$d_q\gamma DN_q$	s_q (LB)	s_q (UB)	$s_{q,w}$
25°	0.0	5.10	9.05	5.87	0.00			
	0.1	10.53	14.88	11.37	4.16	1.30	1.40	1.32
	0.2	15.50	21.06	16.58	7.45	1.40	1.61	1.44
	0.4	25.88	34.54	27.56	13.56	1.53	1.88	1.60
	0.6	37.03	49.21	39.39	19.50	1.64	2.06	1.72
	0.8	48.94	65.37	52.13	25.53	1.72	2.21	1.81
	1.0	61.71	82.94	65.83	31.71	1.79	2.33	1.89
	2.0	138.40	198.80	150.12	64.60	2.06	2.94	2.23
30°	0.0	12.67	21.82	14.49	0.00			
	0.1	23.58	34.50	25.75	7.31	1.49	1.74	1.54
	0.2	33.44	47.44	36.22	13.01	1.60	1.97	1.67
	0.4	54.04	76.94	58.59	23.57	1.76	2.34	1.87
	0.6	76.22	109.35	82.80	33.93	1.87	2.58	2.01
	0.8	100.10	145.60	109.14	44.38	1.97	2.79	2.13
	1.0	125.60	185.41	137.49	54.95	2.06	2.98	2.24
	2.0	280.60	429.60	310.21	111.65	2.40	3.65	2.65
35°	0.0	32.96	58.60	38.61	0.00			
	0.1	55.87	85.73	62.45	13.15	1.74	2.06	1.81
	0.2	76.58	117.27	85.55	23.57	1.85	2.49	1.99
	0.4	119.60	188.92	134.88	42.98	2.02	3.03	2.24
	0.6	165.70	265.33	187.66	61.82	2.15	3.34	2.41
	0.8	215.20	347.35	244.33	80.50	2.26	3.59	2.56
	1.0	268.60	432.52	304.73	99.47	2.37	3.76	2.68
	2.0	594.20	959.73	674.77	201.67	2.78	4.47	3.15
40°	0.0	91.04	184.73	112.84	0.00			
	0.1	143.30	260.76	170.64	25.86	2.02	2.94	2.23
	0.2	190.50	341.83	225.72	46.75	2.13	3.36	2.41
	0.4	287.00	508.50	338.55	84.74	2.31	3.82	2.66
	0.6	391.10	683.55	459.16	121.41	2.47	4.11	2.85
	0.8	502.80	876.80	589.84	158.20	2.60	4.37	3.02
	1.0	622.10	1086.60	730.20	195.34	2.72	4.62	3.16
	2.0	1340.00	2385.20	1583.24	390.71	3.20	5.63	3.76
45°	0.0	277.00	683.09	364.79	0.00			
	0.1	412.40	890.12	515.67	56.18	2.41	3.68	2.69
	0.2	533.80	1111.70	658.73	101.32	2.53	4.23	2.90
	0.4	777.50	1599.56	955.21	184.35	2.71	4.97	3.20
	0.6	1029.00	2121.28	1265.13	264.21	2.85	5.44	3.41
	0.8	1307.00	2667.60	1601.13	343.16	3.00	5.78	3.60
	1.0	1601.00	3234.50	1954.13	421.42	3.14	6.05	3.77
	2.0	3344.00	6577.20	4042.95	821.58	3.73	7.17	4.48

Table 8. Shape and depth factors, s_γ* and d_γ*, for circular, square and rectangular footings.

ϕ	D/B	$q_{bl(2D)}$	d_γ*	Circular		Square		L/B=2		L/B=3	
				q_{bl}	s_γ*	q_{bl}	s_γ*	q_{bl}	s_γ*	q_{bl}	s_γ*
25°	0.0	6.49	1.00	6.22	0.96	5.87	0.90	6.15	0.95	6.28	0.97
	0.1	10.65	1.64	12.14	1.14	11.37	1.07	10.88	1.02	10.80	1.01
	0.2	13.94	2.15	17.61	1.26	16.58	1.19	15.10	1.08	14.69	1.05
	0.4	20.05	3.09	29.09	1.45	27.56	1.37	23.78	1.19	22.54	1.12
	0.6	25.99	4.01	41.61	1.60	39.39	1.52	33.02	1.27	30.80	1.18
	0.8	32.02	4.93	55.09	1.72	52.13	1.63	43.03	1.34	39.66	1.24
	1.0	38.20	5.89	69.81	1.83	65.83	1.72	54.00	1.41	49.23	1.29
30°	0.0	14.75	1.00	15.65	1.06	14.49	0.98	14.94	1.01	14.98	1.02
	0.1	22.06	1.50	27.76	1.26	25.75	1.17	24.03	1.09	23.40	1.06
	0.2	27.76	1.88	38.99	1.40	36.22	1.30	32.24	1.16	30.83	1.11
	0.4	38.32	2.60	62.63	1.63	58.59	1.53	49.57	1.29	46.22	1.21
	0.6	48.68	3.30	88.45	1.82	82.80	1.70	68.40	1.40	62.52	1.28
	0.8	59.13	4.01	116.66	1.97	109.14	1.85	88.83	1.50	79.89	1.35
	1.0	69.70	4.73	147.25	2.11	137.49	1.97	111.04	1.59	98.59	1.41
35°	0.0	34.48	1.00	41.33	1.20	38.61	1.12	37.84	1.10	36.84	1.07
	0.1	47.63	1.38	68.01	1.43	62.45	1.31	56.97	1.20	54.09	1.14
	0.2	58.05	1.68	92.41	1.59	85.55	1.47	74.63	1.29	69.17	1.19
	0.4	77.46	2.25	143.84	1.86	134.88	1.74	111.71	1.44	100.43	1.30
	0.6	96.30	2.79	199.69	2.07	187.66	1.95	150.83	1.57	132.99	1.38
	0.8	114.98	3.33	258.67	2.25	244.33	2.12	193.34	1.68	168.06	1.46
	1.0	133.95	3.88	323.47	2.41	304.73	2.28	239.99	1.79	206.57	1.54
40°	0.0	85.57	1.00	121.45	1.42	112.84	1.32	100.19	1.17	94.41	1.10
	0.1	111.43	1.30	184.61	1.66	170.64	1.53	141.46	1.27	129.80	1.16
	0.2	132.32	1.55	242.56	1.83	225.72	1.71	179.56	1.36	162.30	1.23
	0.4	170.31	1.99	361.46	2.12	338.55	1.99	258.87	1.52	226.05	1.33
	0.6	206.98	2.42	490.93	2.37	459.16	2.22	344.64	1.67	299.72	1.45
	0.8	243.77	2.85	628.18	2.58	589.84	2.42	438.67	1.80	376.67	1.55
	1.0	280.91	3.28	779.86	2.78	730.20	2.60	542.80	1.93	461.57	1.64
45°	0.0	234.21	1.00	398.80	1.70	364.79	1.56	296.19	1.26	275.26	1.18
	0.1	290.39	1.24	568.77	1.96	515.67	1.78	399.94	1.38	364.86	1.26
	0.2	335.53	1.43	724.32	2.16	658.73	1.96	498.41	1.49	448.61	1.34
	0.4	418.56	1.79	1040.75	2.49	955.21	2.28	704.88	1.68	621.22	1.48
	0.6	498.42	2.13	1379.80	2.77	1265.13	2.54	925.73	1.86	800.91	1.61
	0.8	577.37	2.47	1729.87	3.00	1601.13	2.77	1164.91	2.02	991.13	1.72
	1.0	655.63	2.80	2120.67	3.23	1954.13	2.98	1422.37	2.17	1195.08	1.82

LIST OF FIGURES

$$\boldsymbol{\sigma}^l = \left\{ \sigma_{11}^l \;\; \sigma_{22}^l \;\; \sigma_{33}^l \;\; \sigma_{12}^l \;\; \sigma_{23}^l \;\; \sigma_{31}^l \right\}^{\mathrm{T}} ; \;\; l = 1, \ldots, 4$$

$$\boldsymbol{\sigma}^e = \left\{ \sigma_{11}^e \;\; \sigma_{22}^e \;\; \sigma_{33}^e \;\; \sigma_{12}^e \;\; \sigma_{23}^e \;\; \sigma_{31}^e \right\}^{\mathrm{T}}$$

$$\mathbf{u}^l = \left\{ \; u_1^l \, u_2^l \, u_3^l \right\}^{\mathrm{T}} ; \;\; l = 1, \ldots, 4$$

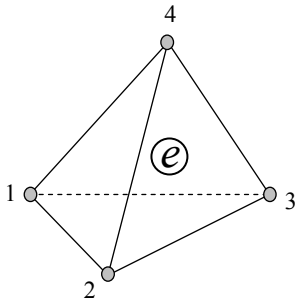

(a) Lower bound finite element.

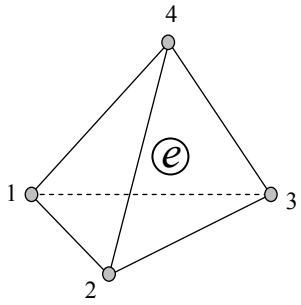

(b) Upper bound finite element.

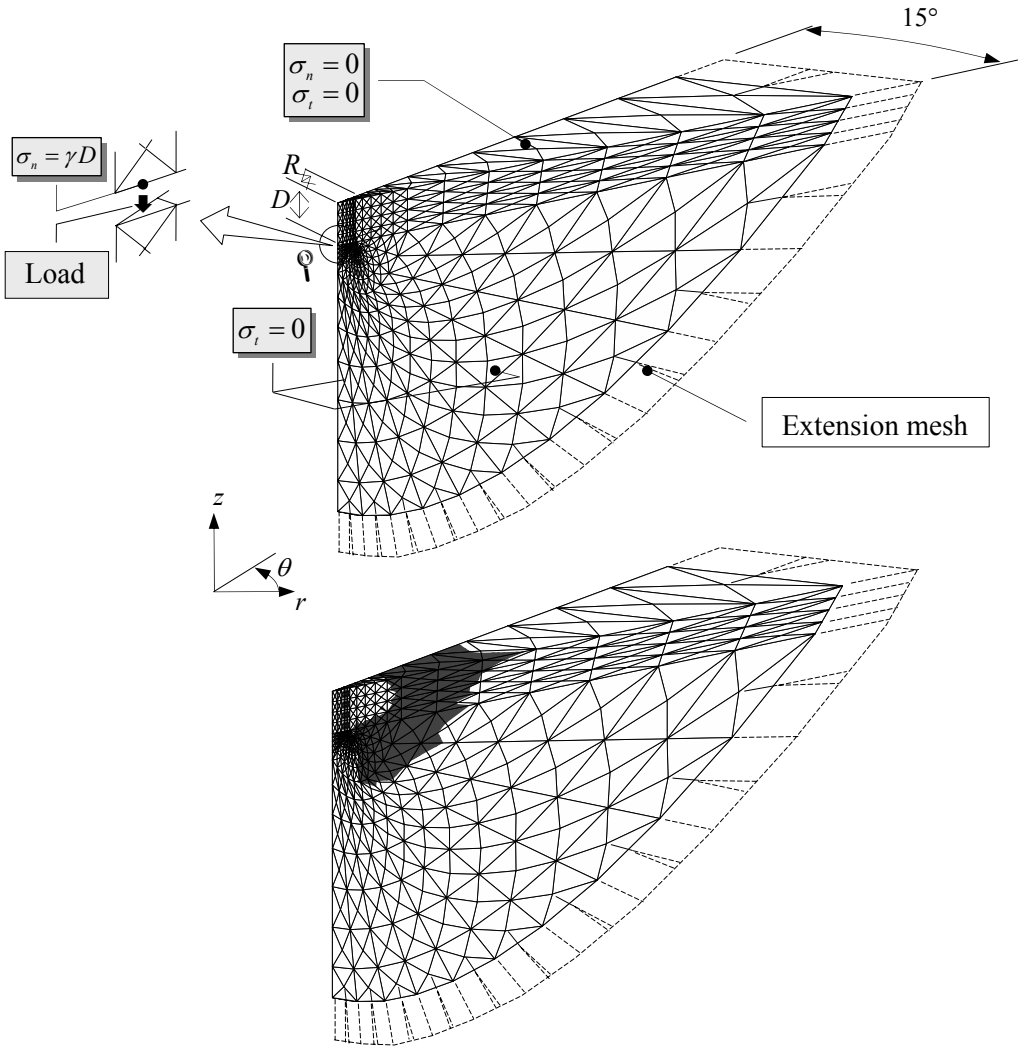
15°
$\sigma_n = 0$
$\sigma_t = 0$
$\sigma_n = \gamma D$
R
D
Load
$\sigma_t = 0$
Extension mesh
z
θ
r

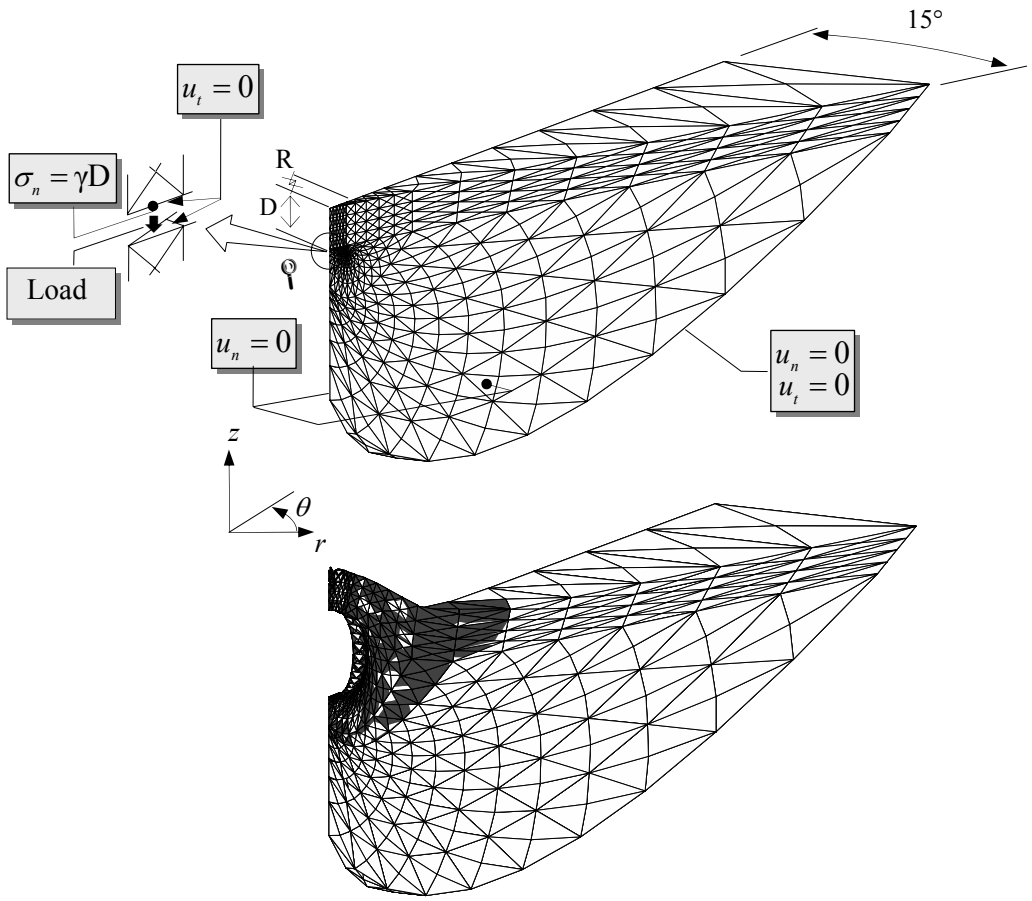
15°
$u_t = 0$
$\sigma_n = \gamma D$
R
D
Load
$u_n = 0$
$u_n = 0$
$u_t = 0$
z
θ
r

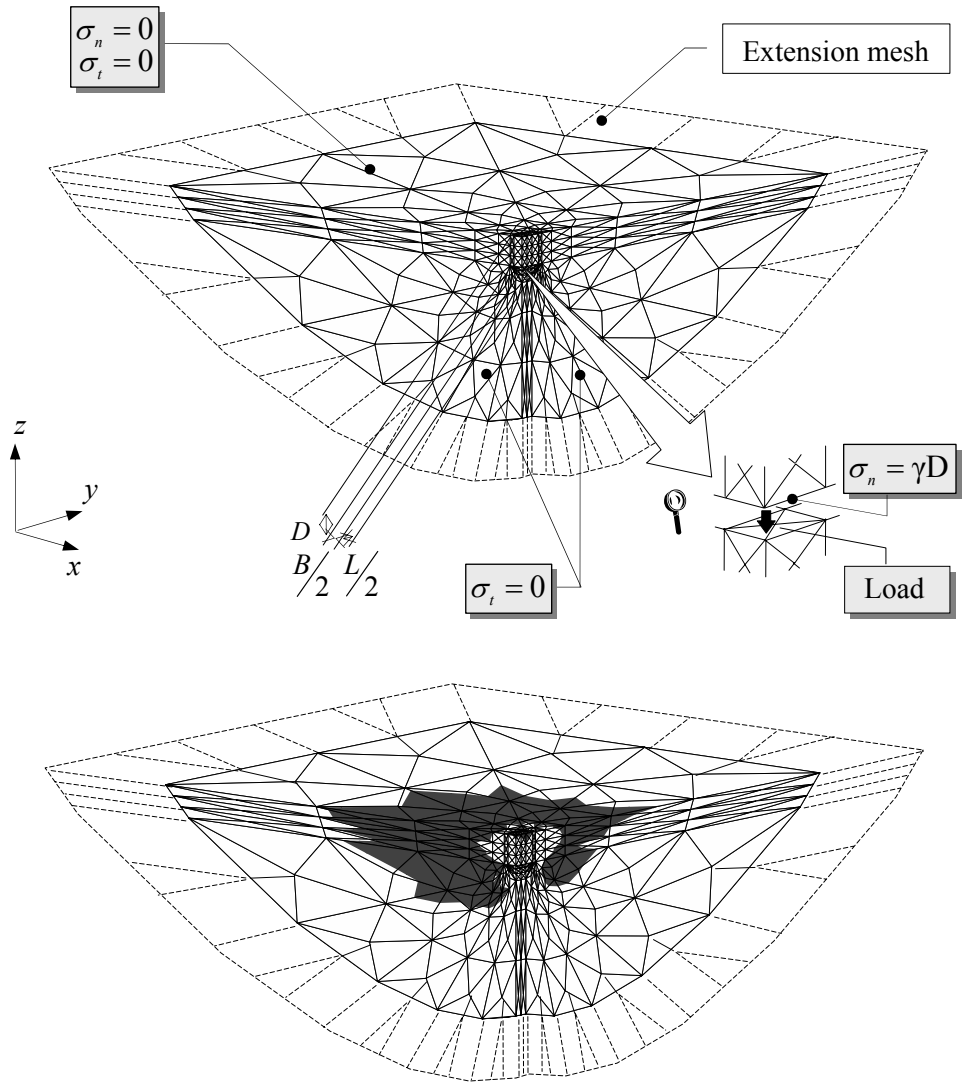
$\sigma_n = 0$
$\sigma_t = 0$
Extension mesh
z
y
x
D
B/2
L/2
$\sigma_t = 0$
$\sigma_n = \gamma D$
Load

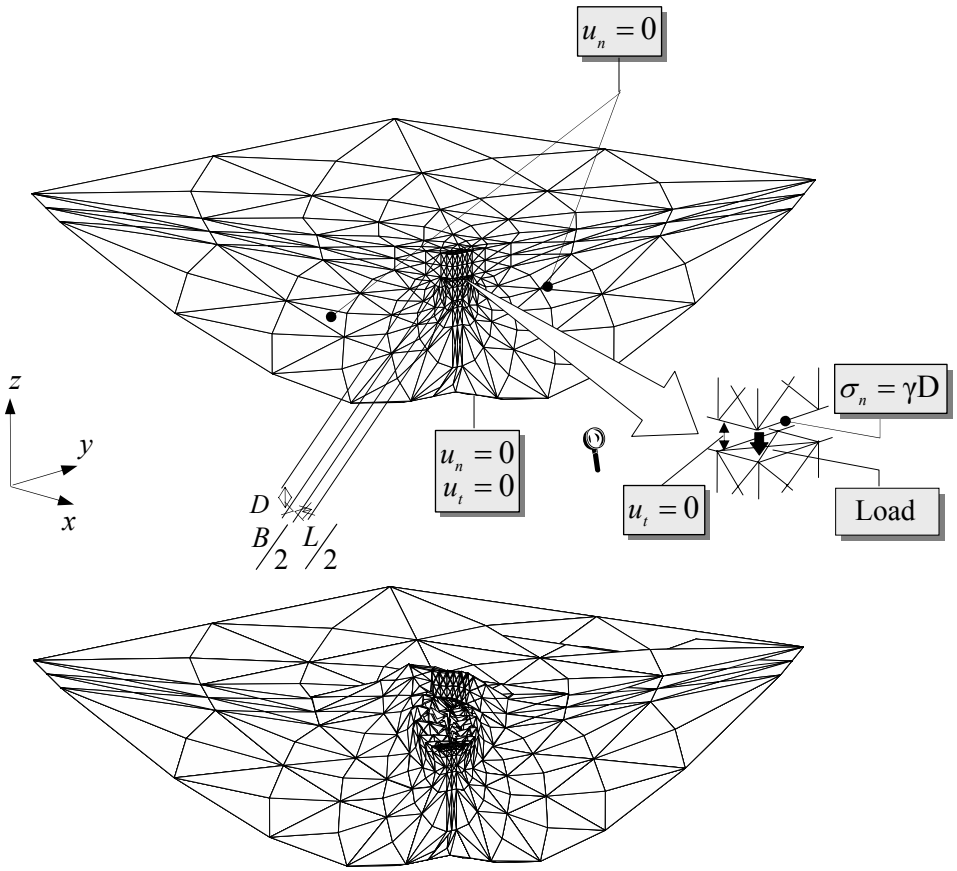
$u_n = 0$
$\sigma_n = \gamma D$
$u_n = 0$
$u_t = 0$
$u_t = 0$
Load
z
y
x
D
B/2
L/2

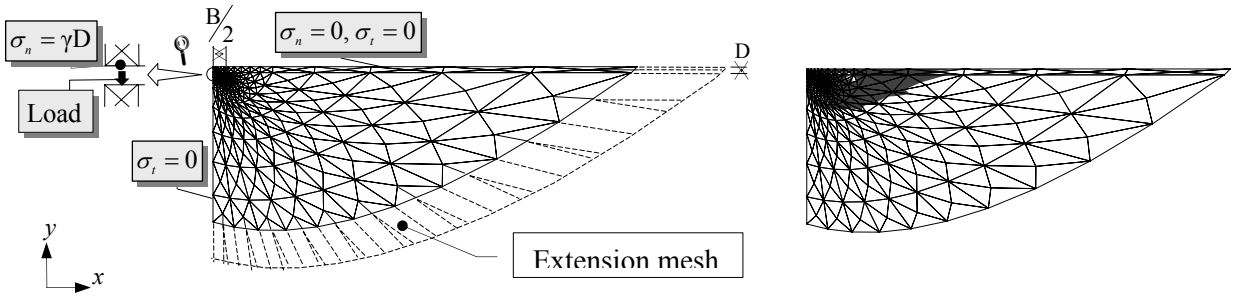

(a) D/B=0.2

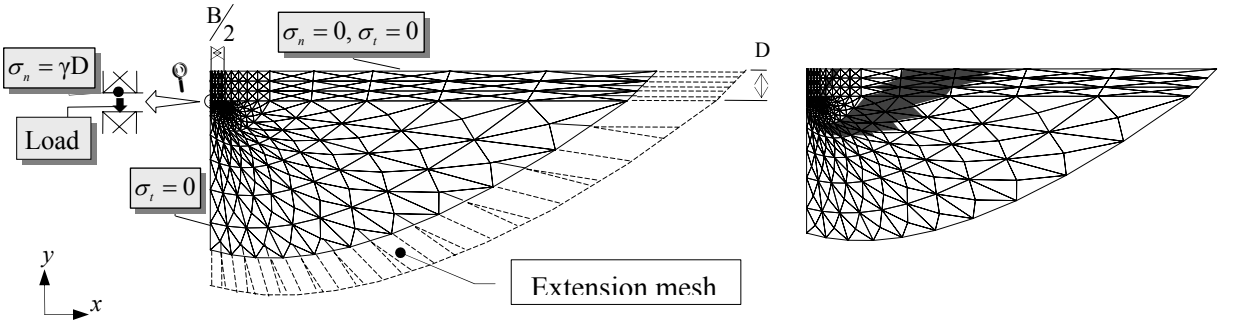

(b) D/B=1.0

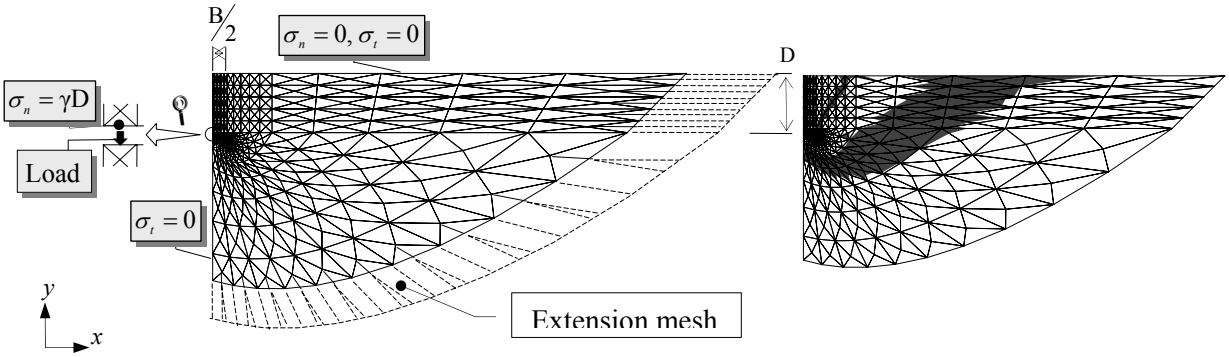

(c) D/B=2.0

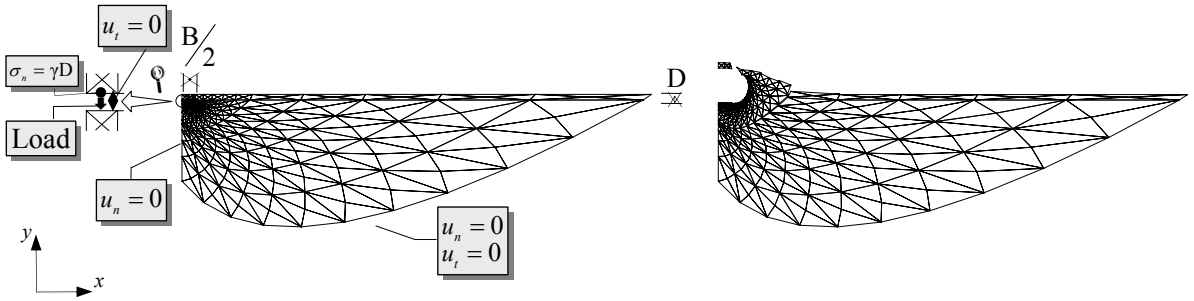

(a) D/B=0.2

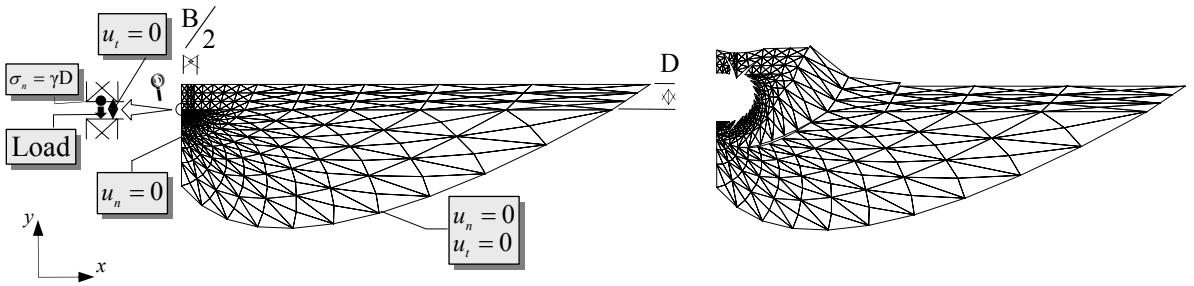

(b) D/B=1.0

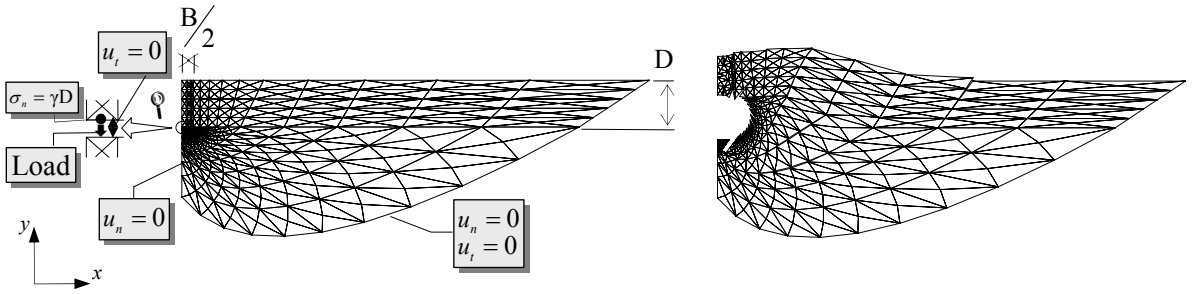

(c) D/B=2.0

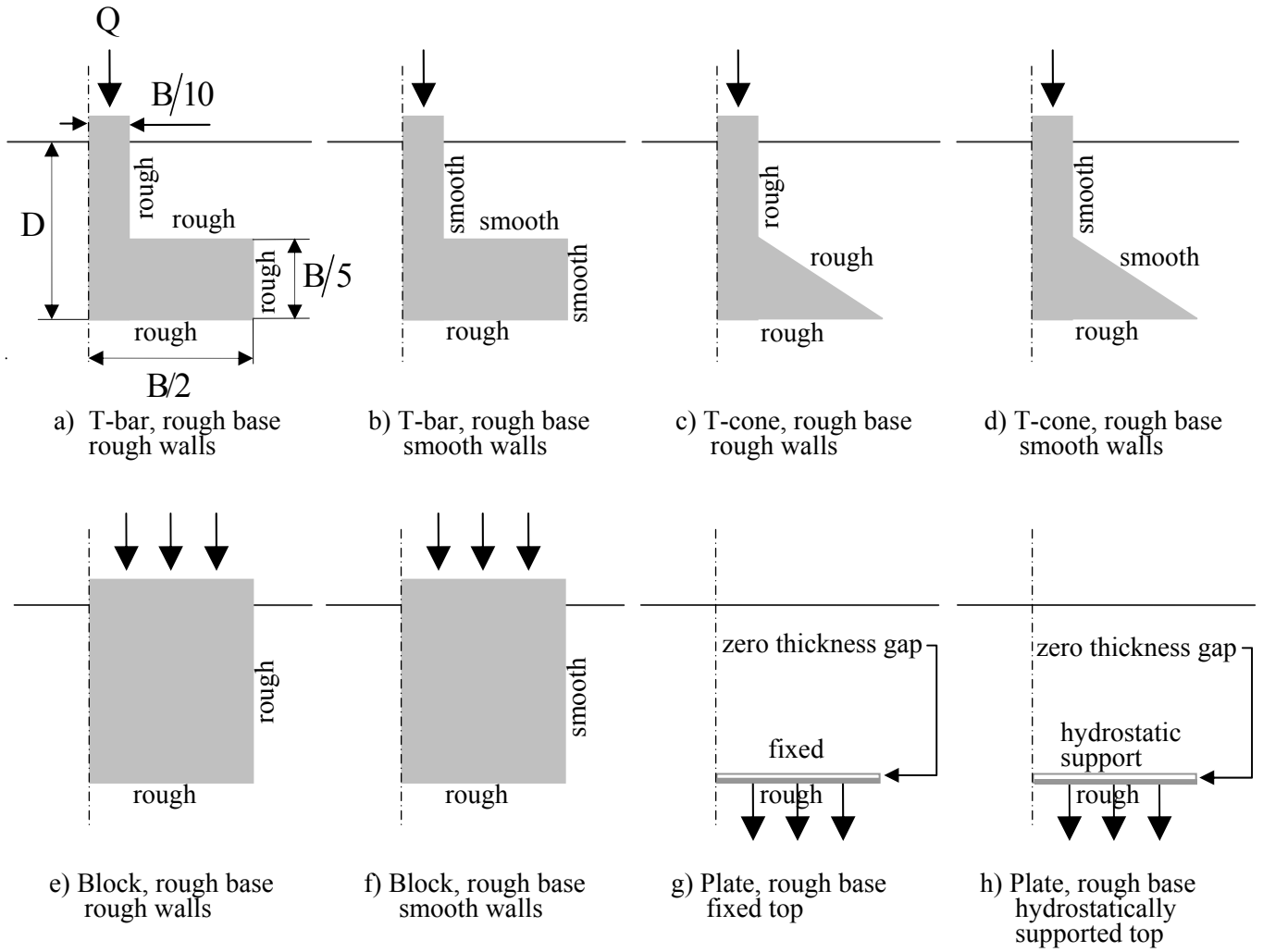

a) T-bar, rough base rough walls

b) T-bar, rough base smooth walls

c) T-cone, rough base rough walls

d) T-cone, rough base smooth walls

e) Block, rough base rough walls

f) Block, rough base smooth walls

g) Plate, rough base fixed top

h) Plate, rough base hydrostatically supported top

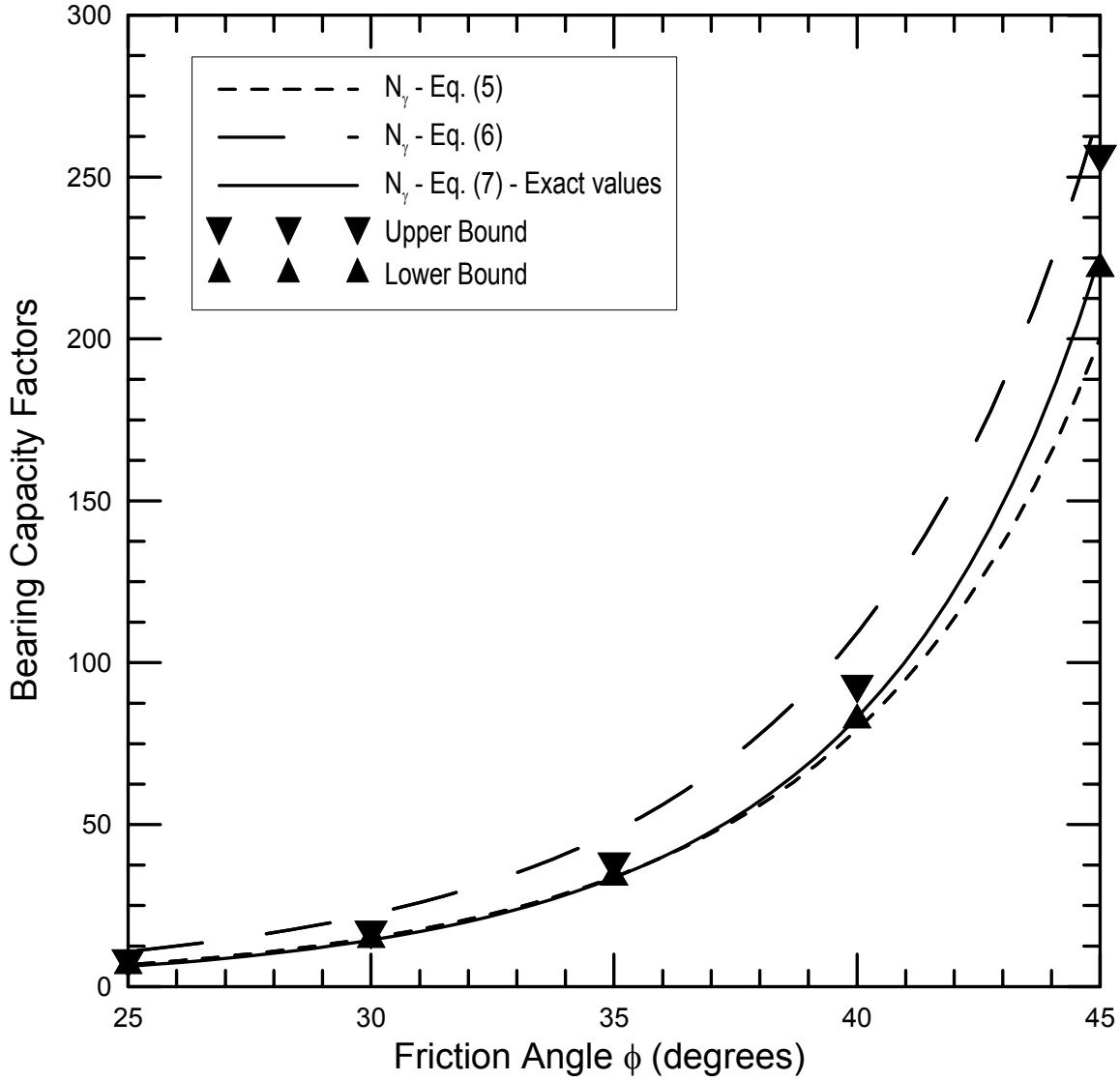
300
250
200
150
100
50
0
25
30
35
40
45
Bearing Capacity Factors
Friction Angle ϕ (degrees)
N_γ - Eq. (5)
N_γ - Eq. (6)
N_γ - Eq. (7) - Exact values
Upper Bound
Lower Bound

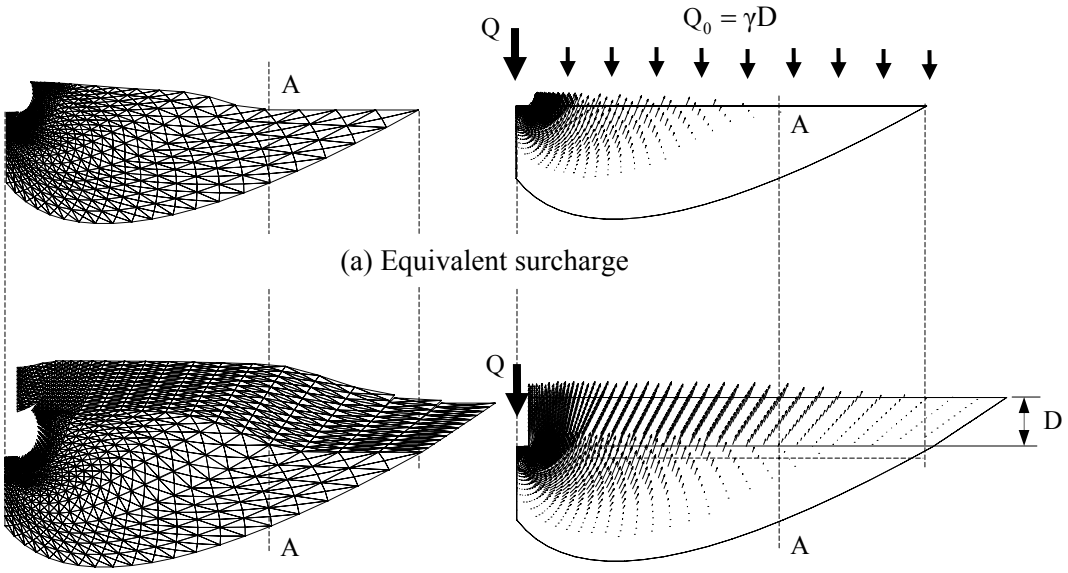

(a) Equivalent surcharge

(b) Embedded footing

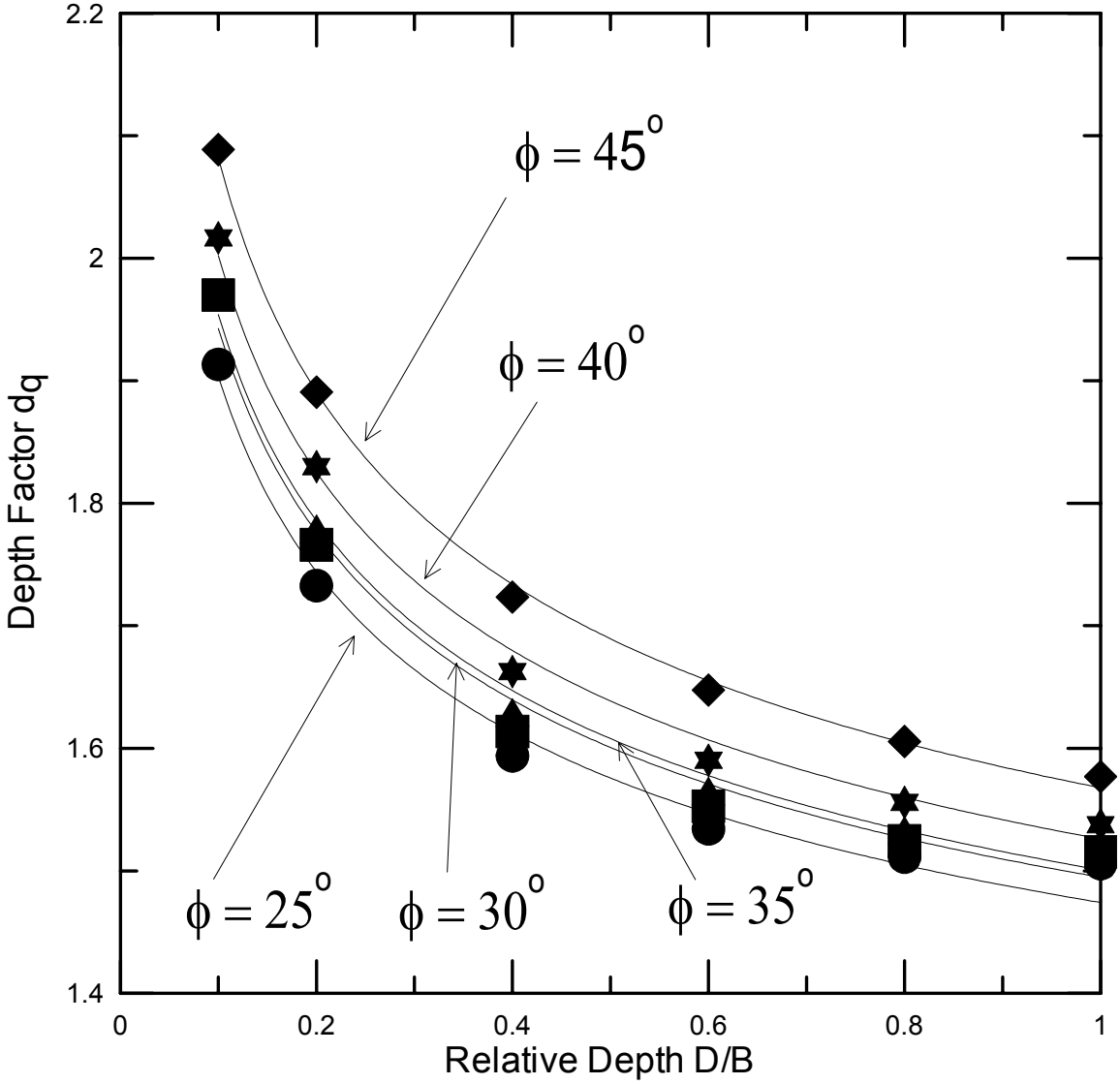
2.2
2
1.8
1.6
1.4
Depth Factor dq
0
0.2
0.4
0.6
0.8
1
Relative Depth D/B
ϕ = 45°
ϕ = 40°
ϕ = 25°
ϕ = 30°
ϕ = 35°

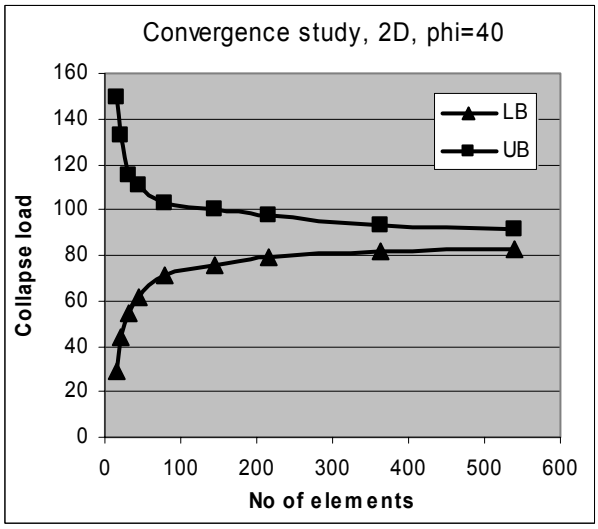

(a) Convergence rates for strip footing

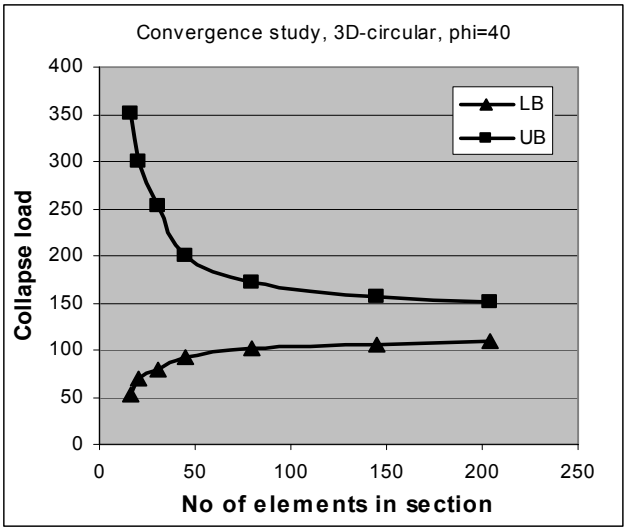

(b) Convergence rates for circular footing

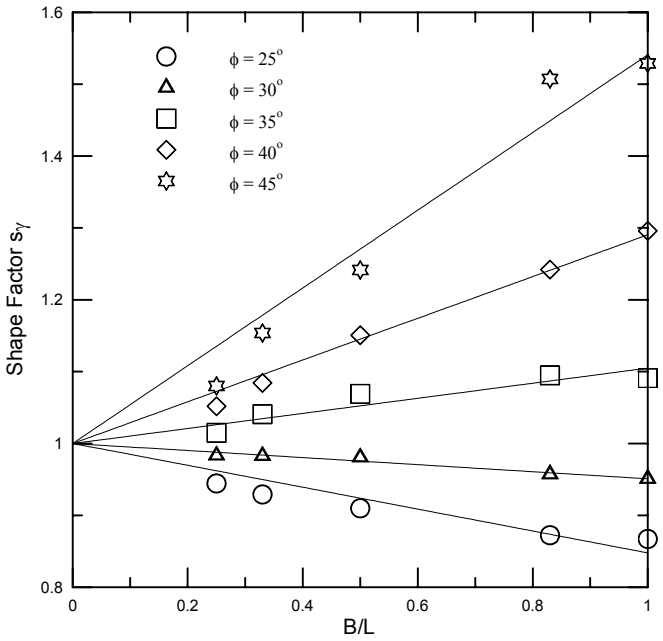
1.6
1.4
1.2
1
0.8
0
0.2
0.4
0.6
0.8
1
B/L
Shape Factor s_γ
$\phi = 25^o$
$\phi = 30^o$
$\phi = 35^o$
$\phi = 40^o$
$\phi = 45^o$

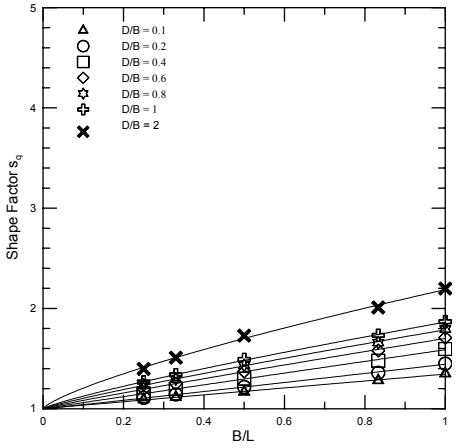
D/B = 0.1
D/B = 0.2
D/B = 0.4
D/B = 0.6
D/B = 0.8
D/B = 1
D/B = 2
Shape Factor s_q
B/L

(a)

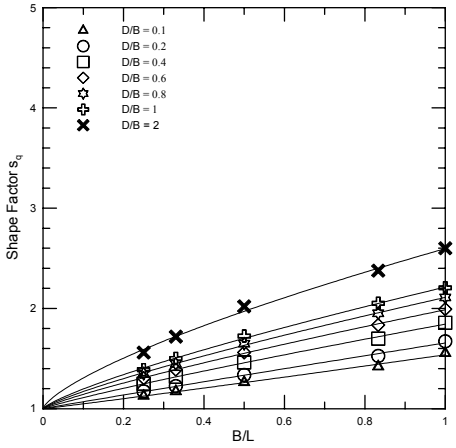
D/B = 0.1
D/B = 0.2
D/B = 0.4
D/B = 0.6
D/B = 0.8
D/B = 1
D/B = 2
Shape Factor s_q
B/L

(b)

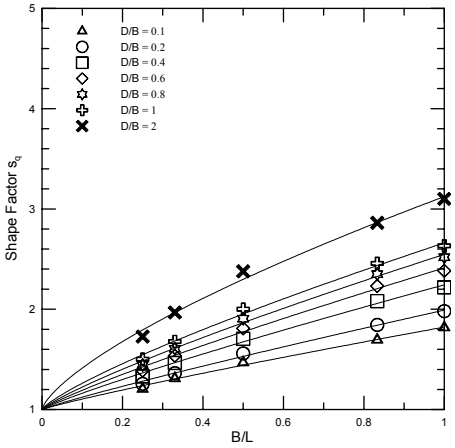
D/B = 0.1
D/B = 0.2
D/B = 0.4
D/B = 0.6
D/B = 0.8
D/B = 1
D/B = 2
Shape Factor s_q
B/L

(c)

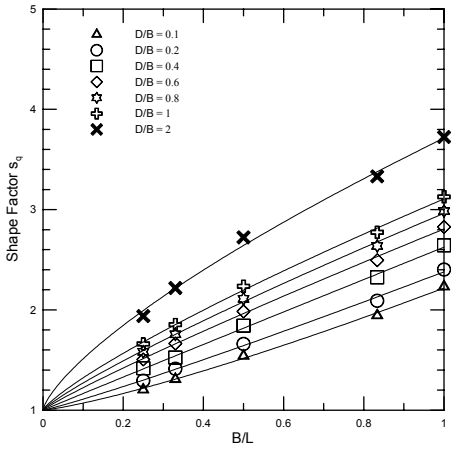
D/B = 0.1
D/B = 0.2
D/B = 0.4
D/B = 0.6
D/B = 0.8
D/B = 1
D/B = 2
Shape Factor s_q
B/L

(d)

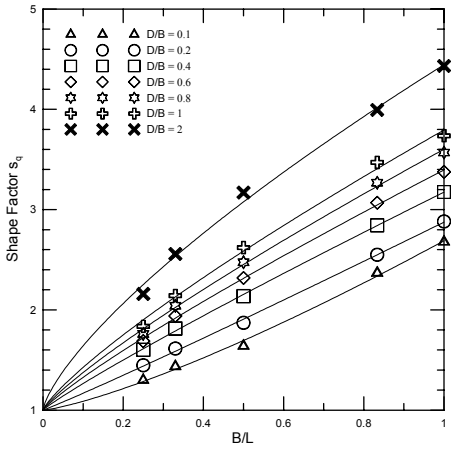
D/B = 0.1
D/B = 0.2
D/B = 0.4
D/B = 0.6
D/B = 0.8
D/B = 1
D/B = 2
Shape Factor s_q
B/L

(e)

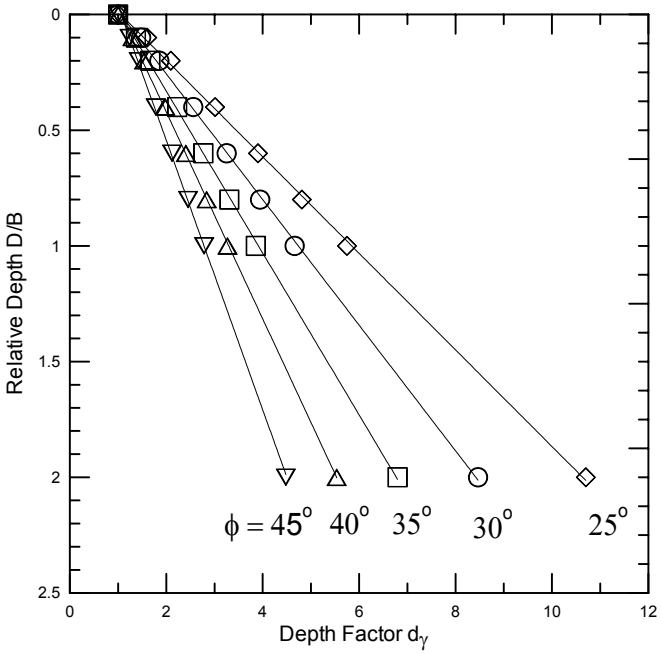
Relative Depth D/B
Depth Factor d_γ
$\phi = 45^o$ 40^o 35^o 30^o 25^o
0
0.5
1
1.5
2
2.5
0
2
4
6
8
10
12